Equivalent electron correlations in nonsequential double ionization of noble atoms*

Shansi Dong(董善思)[1], Qiujing Han(韩秋静)[2], and Jingtao Zhang(张敬涛)[1,†]

[1] *Department of Physics, Shanghai Normal University, Shanghai* 200234, *China*

[2] *Qingdao Binhan University, Qingdao* 266555, *China*

(Received 8 September 2016; revised manuscript received 27 October 2016; published online 20 December 2016)

Electron correlation is encoded directly in the distribution of the energetic electrons produced in a recollision-impact double ionization process, and varies with the laser field and the target atoms. In order to get equivalent electron correlation effects, one should enlarge the laser intensity cubically and the laser frequency linearly in proportion to the second ionization potentials of the target atoms. The physical mechanism behind the transform is to keep the ponderomotive parameter unchanged when the laser frequency is enlarged.

Keywords: scaling law, electron correlation, double ionization

PACS: 32.80.Rm, 32.80.Fb, 34.50.Rk, 42.50.Hz **DOI:** 10.1088/1674-1056/26/2/023202

1. Introduction

The electron correlation effect lies in the core of atto-science and molecular bonding, and is also important to the study of electron motion in chemical reactions.[1,2] Double ionization of atoms in intense laser fields provides a simple electron correlation prototype and thus becomes a hot topic in the study of atom–light interaction. Studies on double ionization have revealed many electron correlation features, such as the effect of single and multiple recollisions of two electrons, the timing of electron releases in sequential double ionization, and momentum–energy redistribution among electrons.[1]

Nonsequential double ionization (NSDI) of noble atoms[3] discloses an electron correlation process during photoionization that one electron is firstly ionized by the laser field, then is driven back to its parent ion and finally knocks out another electron. Clearly, the electron correlation plays a key role in NSDI.[4,5] Correlated-electron momentum distribution (CMD) is a principal tool to reveal the electron correlation effect in NSDI and is frequently studied. The CMD denotes the number of two electrons as a function of their momenta along the laser polarization. Many features, such as the fingerlike structure[6] and the cross-shape structure[7,8] in the CMDs, are observed experimentally and analyzed theoretically. These structures bring detailed information of microscopic electronic processes. Recently, the experimentally observed transition of CMD from anticorrelation to correlation[9] was found to be caused by the variation of the electron correlation effect with laser intensity.[10]

Scaling technique is a valuable tool to analyze many physical processes and is frequently used to study the intense-laser phenomena.[11–15] Different from the focus on the yield variation with the laser wavelength,[11,13] we conclude a scaling law to identify the equivalent electron processes in NSDI,[16] by the similarity of CMDs of two electrons ionized from different atoms. The scaling law states that for two systems of laser-driven atoms S (ω, I, I_{p2}) and S$'$ (ω', I', I'_{p2}), their CMDs are the same provided that we choose $\omega' = \omega * (I'_{p2}/I_{p2})$ and $I' = I * (I'_{p2}/I_{p2})^3$, where ω and I are the frequency and intensity of the laser field, and I_{p2} is the second ionization potential of the atom, and the quantities with primes denote those for another system. The scaling law suggests that, under the scaling transform, the principal electronic processes of NSDI are the same, even though the laser parameters look quite different. The NSDI process can be further classified into two categories,[17] say recollision-impact-ionization (RII) and recollision-induced excitation with subsequent ionization (RESI) processes. In the RII process, the second electron is ionized owing mainly to the electron recollision, while the second electron in the RESI process is ionized by the laser field from an excited state. Hence, the change of their CMDs with the laser field may be quite different. Do the two processes satisfy the same scaling law?

Moreover, the electron correlation is encoded directly into the CMDs of the RII electrons. This can be shown by the drift momentum that the electron obtains when it moves in the laser field. For given laser intensity and frequency, the drift momentum depends critically on the time of electron ionization, hence the drift momenta of two RII electrons are almost

*Project supported by the National Natural Science Foundation of China (Grant Nos. 61475168 and 11674231) and sponsored by Shanghai Gaofeng & Gaoyuan Project for University Academic Program Development (Zhang).

†Corresponding author. E-mail: jtzhang@shnu.edu.cn

© 2017 Chinese Physical Society and IOP Publishing Ltd

the same, since the two electrons were freed with a short time interval.[18] The first electron is ionized during the increasing edge of the electric field, and recollides with the parent core at the zero-crossing point of the electric field.[18] The return generally takes a half cycle, and the recollision inverses the momentum of the first electron. Consequently, the time of recollision can be regarded as the ionization time of the first electron. Hence, the drift momenta are almost the same for two electrons in the RII process. As a result, the end-of-pulse CMD of the RII electrons keeps a direct memory of the CMD at the moment of the electron collision. This presents a straightforward way to study the electron correlation in the NSDI process. According to the change of CMDs of the RII electrons, one gets the variation of the electron correlation. Because the electron correlation lies in the core of NSDI study, further study focussing on the CMDs of the RII electrons is of great importance.

In this paper, we study the CMDs of the RII electrons under the scaling transform. This paper serves two purposes. One is to show the scaling law in the RII process, the other, which is more important, is to check the change of the electron correlation under the scaling transform. For these purposes, we calculate the CMDs in the laser fields of different frequencies and intensities using a classical ensemble method. We will show that, under the scaling transform, the CMDs of the RII electrons are the same. The similarity in the CMDs indicates that equivalent electron correlations are ensured under the scaling transform.

2. Simulation method

The simulation method we employed is based on the numerical integration of the time-dependent Newton equation, which has been proved to be very effective in dealing with the NSDI phenomena.[19–21] This method reproduced many important features in NSDI, such as the multi-peak structure in momentum distributions of ions from single, double and multiple ionizations,[22] and the characteristic knee structure in the ion yield by circular polarization.[23] Moreover, by back-trajectory technique, this method can be used to track subcycle electronic dynamics during double ionization.[24–26]

The light-free Hamiltonian of a two-active-electron atom can be written as (in atomic units: a.u.):

$$H_{\rm e} = \sum_{i=1,2}\left[\frac{\boldsymbol{P}_i^2}{2} - 2V_{\rm sc}(r_i,a)\right] + V_{\rm sc}(\boldsymbol{r}_1-\boldsymbol{r}_2,b), \qquad (1)$$

where $\boldsymbol{r}_i$ and $\boldsymbol{p}_i$ denote, respectively, the position and momentum of the i-th electron; $V_{\rm sc}$ stands for the soft-core Coulomb potential defined as $V_{\rm sc}(\boldsymbol{r},c) = (r^2+c^2)^{-0.5}$. The initial position space collection of two electrons is populated by a Gaussian random series ensuring the total kinetic energy positive in Eq. (1). These electrons move freely for enough time until they keep the stable position and momentum distribution. Then we get the initial state of the ensemble.

The Hamiltonian of the atom in a laser pulse is given by

$$H = H_{\rm e} + (\boldsymbol{r}_1+\boldsymbol{r}_2)\cdot\boldsymbol{E}(t),$$

where $\boldsymbol{E}(t)$ is the electric field of the laser pulse. For linear polarization it can be written as:

$$\boldsymbol{E}(t) = E_0 f(t)\cos(\omega t)\hat{\boldsymbol{x}},$$

where E_0 and ω are the laser amplitude and frequency, respectively, $f(t)$ denotes the pulse envelope, and $\hat{\boldsymbol{x}}$ is a unit vector along the x direction. In our simulation, the pulse envelope is chosen as a 16-cycle trapezoidal shape with 3 cycles in both the ramp on and the ramp off. The motion of two electrons in the laser field is governed by the canonical equation as:

$$\frac{{\rm d}\boldsymbol{r}_i}{{\rm d}t} = \frac{\partial H}{\partial \boldsymbol{p}_i}, \quad \frac{{\rm d}\boldsymbol{p}_i}{{\rm d}t} = -\frac{\partial H}{\partial \boldsymbol{r}_i}. \qquad (2)$$

The above equation is solved by using the standard 4-5th Runge–Kutta algorithm. At the end of the pulse, a double ionization event is counted when the energy of each electron is greater than zero. A CMD is obtained statistically on all double ionization events.

In our simulations, we separate the RII from the NSDI by the time interval between the recollision time and the double ionization time. The double ionization events with the time interval less than 0.1 optical cycle are counted as the RII events, while the double ionization events with the time interval larger than 0.3 optical cycle are counted as the RESI events. By the back-trajectory technique, the contribution of the RII and RESI electrons to NSDI can be identified. Figure 1(a) depicts a CMD of two electrons from the NSDI process of the Ar atom. The CMD exhibits large cyan bright regions in the center of a blue background, and small red structures highlighted from the bright regions. The bright regions distribute mainly along the diagonal line of the plot, indicating electrons accumulated greatly in the first and the third quadrants. Figure 1(b) depicts the CMD of two electrons from the RESI process, which exhibits the bright regions along the two axes and the red structures in the central area of the plot. Figure 1(c) depicts the CMD of the RII electrons, in which the bright areas appear only in the first and the third quadrants, and the red structures keep away from the center. This demonstrates that most RII electrons are energetic and form the structures far away from the center, and that the RESI electrons form the structures nearby the center. Therefore, we focus on these energetic electrons to get deep insight into the electron correlation effect.

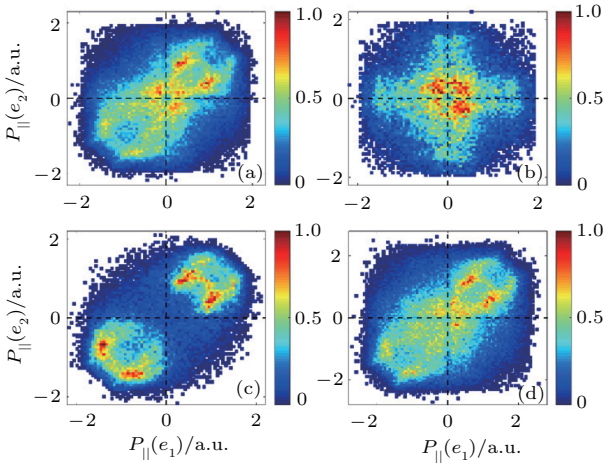


Fig. 1. (color online) CMDs of two electrons ionized from Ar atoms in laser pulse of wavelength 795 nm and intensity 3.0×10^{14} W/cm^2: (a) NSDI, (b) RESI, and (c) RII processes, and the CMD from Ne atoms in laser pulses of wavelength 536 nm and intensity 9.77×10^{14} W/cm^2 (d). All the laser pulses are of 16-cycle trapezoidal shape with 3 cycles in both linear ramp on and linear ramp off.

3. scaling relation for RII

The scaling law originates from the fact that the transition amplitude of an electron is described by Bessel functions.[27] It was deduced originally from single-electron photoionization of atoms,[28–30] and was extended to high-order harmonic generation.[31] If we regard the two electrons in double ionization as a whole, its transition can also be described by Bessel functions. This suggests a scaling law for double ionization. Actually, the Bessel functions appear in the analytical formula of the double ionization rate.[32] The key of the scaling transform is to keep the ponderomotive parameter unchanged. When the laser frequency changes to $k\omega$, the laser intensity should be changed as $k^3 I$, so the ponderomotive parameter defined as $u_p = I/4\omega^3$ keeps constant. A comparison is presented in Fig. 1. The CMD shown in Fig. 1(d) is for Ne atom with $k = 1.482$, i.e., the ratio of the second ionization potentials. According to the bright areas and the red structures, the similarity between Fig. 1(a) and Fig. 1(d) is evident, which proves the scaling law of NSDI. This verifies that the ponderomotive parameter is a basic parameter in strong laser fields.

Does the electron correlation change under the scaling transfer? To answer this question, we study the CMDs of two RII electrons. We choose the CMD from the Ar atoms as a reference and compare the CMDs of the RII electrons under the scaling transform. Figure 2(a) depicts a CMD of two electrons from RII of the Ar atom. The bright areas locate at the first and the third quadrants. These areas are symmetrically located about the diagonal line, indicating the fact that two electrons are not distinguishable. In the first quadrant, the bright area disperses a little, hence becomes closer to the two axes. This area is not so highlighted as that in the third quadrant. This difference is caused by the ionization saturation at the leading pulse edge and becomes faint at lower laser intensities. Less electrons emit out back-to-back, hence the areas in the second and the fourth quadrants appear as a blue background. Such a distribution denotes the two electrons leaving the laser field mainly side-by-side, and is termed as correlation. This plot behaves as a reference to compare the CMDs of two electrons from other atoms.

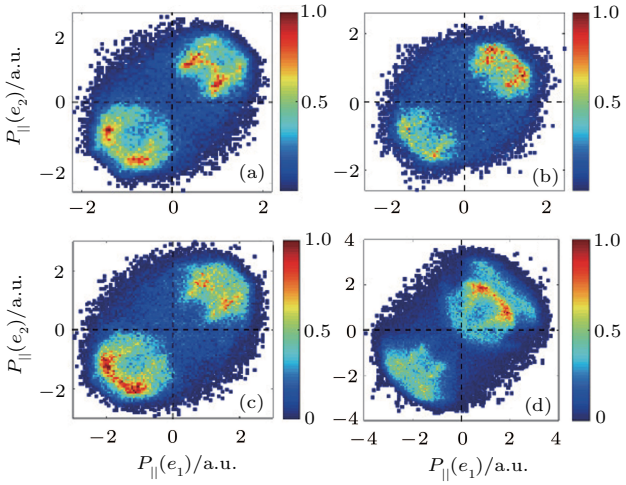


Fig. 2. (color online) CMDs of two electrons from RII of (a) Ar atoms in laser pulses of wavelength $\lambda = 795$ nm and intensity $I_0 = 3.0 \times 10^{14}$ W/cm^2; and He atoms in laser pulses of wavelength 403 nm and intensity 1.16×10^{15} W/cm^2 (b), 2.29×10^{15} W/cm^2 (c), and 4.52×10^{15} W/cm^2 (d), respectively. The scaling ratio is 1.97.

We compare the above CMD with those from the He atoms to choose equivalent electron correlation processes in different laser fields. He atoms are a frequently studied target in NSDI. The scaling transform is featured by the cubic dependence of the laser intensity on the scaling ratio, so we compare the CMDs from the He atom driven by laser intensity k^2, k^3, and k^4, respectively. The scaling ratio k is chosen as the ratio of the second ionization potentials and reads 1.97, so the wavelength of the driving laser field is chosen as 403 nm. The calculated CMDs are depicted in Figs. 2(b), 2(c), and 2(d), respectively. All the CMDs exhibit the bright areas located in the first and the third quadrants, indicating the side-by-side emission being dominated. According to the bright areas and the red structures, the differences from the referential CMD are notable in the calculated CMDs shown in Figs. 2(b) and 2(d), and the similarity with the referential one is substantial in the CMD shown in Fig. 2(c). Figure 2(c) is for laser intensity of $k^3 I_0$, so the similarity demonstrates the cubic dependence of the laser intensity on the scaling ratio.

For a substantial proof of the scaling law, we compare the momentum distributions of the recoil ions. The momentum distribution denotes the number of ions as a function of the recoil momentum along the laser polarization. It presents a quantitative statistic on the ions' motion and thus provides a

cross evidence to the emission of electrons. Figure 3(a) depicts the momentum distributions of the recoil ions corresponding to Fig. 2. The black line is for the Ar^{2+} ion, and the other three lines are for the He^{2+} for different laser intensities. All the lines exhibit two peaks located symmetrically about the central zero. This kind of distribution denotes that almost half of ions move in one direction and the other half of ions move in the opposite direction. Since the two electrons eject side-by-side, the recoil momentum of ion is large. The green line is for the laser intensity k^3I_0 and agrees best with the referential line, while the red (for k^2I_0) and the blue (for k^4I_0) lines exhibit distinctive differences from the referential line.

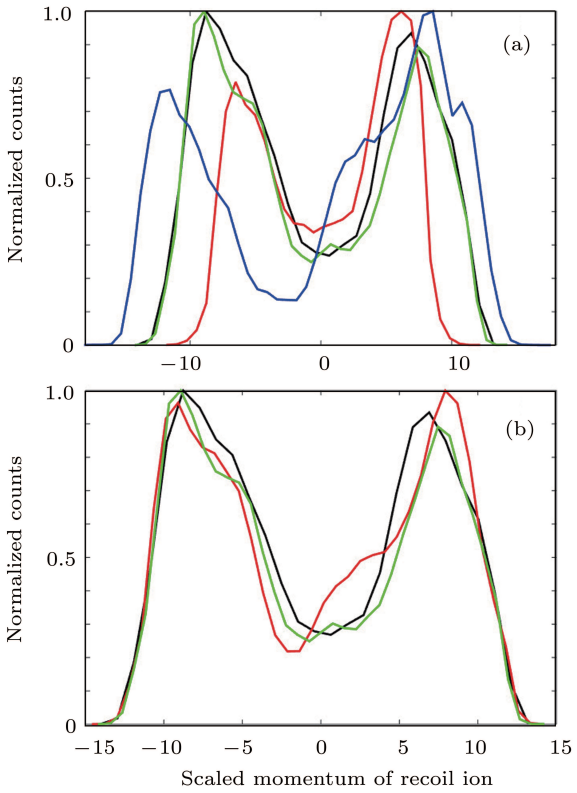


Fig. 3. (color online) Momentum distributions of the recoil ions: The black line is for Ar^{2+} ions produced in a laser field of wavelength $\lambda = 795$ nm and intensity $I_0 = 3.0 \times 10^{14}$ W/cm^2, and other lines are for He^{2+} ions: (a) by laser fields of wavelength 403 nm and intensity 1.16×10^{15} W/cm^2 (red), 2.29×10^{15} W/cm^2 (green), and 4.52×10^{15} W/cm^2 (blue), respectively; (b) by laser fields of wavelength λ/k and intensity k^3I_0 for $k = k_+$ (red) and $k = k_2$ (green), respectively. For convenience of comparison, each line is normalized by its maximum, and the momentum is normalized by $\sqrt{\omega}$.

Is the ratio of the second ionization potentials the best scaling ratio? The scaling ratio is defined as the ratio of ionization potentials of two atoms, which is obvious and specific for single ionization. However, both the first and the second ionization potentials are involved in double ionization, and they combine four ratios as $k_i = I_{pi}/I'_{pi}$ where $i = 1, 2$, and $k_\pm = (I_{p1} \pm I_{p2})/(I'_{p1} \pm I'_{p2})$, where I_{p1} and I_{p2} denote the first and the second ionization potentials of one atom, and the prime denotes the other atom, respectively. The ratio k_+ is straightforward according to the energy relation in double ionization, and the ratio k_- is meaningful if we regard double ionization as the ionization of a two-level atom. We calculate the CMDs of two electrons from RII of the He atom for different ratios. The wavelength of the laser field is chosen as λ/k and the intensity is chosen as k^3I_0. All the calculated CMDs exhibit two bright areas surrounded by the blue background, and the bright areas in four plots all locate at the first and the third quadrants and all keep away from the central regions. The similarity stems from the fact that the ponderomotive parameter, say u_p, is the same in these four plots. The differences are subtle. In Figs. 4(a) and 4(b), which are for k_1 and k_+, respectively, the bright areas in the first quadrant are larger than those in the third quadrant, and the red structures are quite dim. Those notable differences from the referential one exclude k_1 and k_+ as the best scaling ratio. The CMD shown in Fig. 4(d) is for k_- and differs notably from the referential one, especially in the third quadrant. This indicates that k_- is not the proper scaling ratio. However, the difference for the CMD in Fig. 4(c) from the referential one is quite subtle, hence we judge that k_2 is the best scaling ratio. For substantial proof, we compare the momentum distributions of He^{2+} ions for k_2 and k_+ with that of Ar^{2+} ions in Fig. 3(b). Distinctive differences are found for the k_+ line from the referential line, which proves again k_2 is the best scaling ratio.

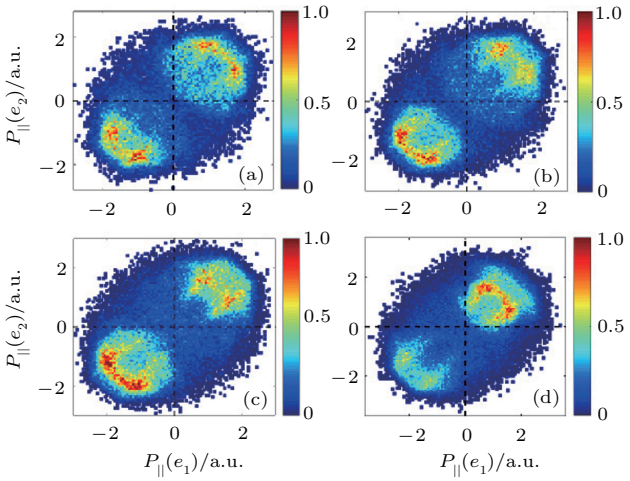


Fig. 4. (color online) CMDs of two electrons from RII of He atoms in laser pulses of wavelength λ/k nm and intensity k^3I_0 for different k: (a) $k = k_1$, (b) $k = k_+$, (c) $k = k_2$, and (d) $k = k_-$, respectively.

Why does the scaling ratio equal the ratio of the second ionization potentials? In double ionization, the second electron should have sufficient energy to overcome the second ionization potential for its ionization. For target atoms with larger second ionization potentials, the energy of the second electron should be enlarged in proportion. The energy of the returning electron depends on the laser intensity, and reaches a maximum of about $3.2U_p$, where U_p is the ponderomotive energy and $U_p = u_p\omega$. During collision, the second electron shares this energy with the returning electron. So, the energy

of the second electron obtained depends on the ponderomotive energy. Because the ponderomotive parameter u_p keeps unchanged under the scaling transform, the laser frequency should be enlarged according to the ratio of the second potentials. Hence, the scaling ratio equals the ratio of the second ionization potentials. This also indicates that both the RII and the RESI processes satisfy the same scaling law as that in the NSDI process.

4. Conclusions

Using a classical ensemble method, we study the CMDs of two RII electrons that keep direct memory of the electron correlation effect. We find that the CMDs of the RII process, as well as the electron correlation effect, satisfy the same scaling law as that in the NSDI process. This indicates that the scaling law of the NSDI process is generally in the two-electron process. Under the scaling transform, many electron correlation processes, such as the energy sharing in electron-electron collision and the electron ejection from the laser field, are the same. The scaling law presents a tool to compare different colliding processes for different atoms, and a way to identify equivalent electron-electron colliding processes. We conclude that in order to get equivalent electron correlation effects, one should choose laser fields of equal ponderomotive parameter, and the laser frequency should be changed in linear proportion to the second ionization potentials of the target atoms. This study presents a deep insight into the electron correlation during NSDI.

References

[1] Becker W, Liu X, Ho P and Eberly J H 2012 *Rev. Mod. Phys.* **84** 1011
[2] Xie X, Lostedt E, Roither S, Schofler M, Kartashov D, Midorikawa K, Baltuška A, Yamanouchi K and Kitzler M 2015 *Sci. Rep.* **5** 12877
[3] Talebpour A, Larochelle S and Chin S L 1997 *J. Phys. B: At. Mol. Opt. Phys.* **30** L245
[4] Weber T H, Giessen H, Weckenbrock M, Urbasch G, Staudte A, Spielberger L, Jagutzki O, Mergel V, Vollmer M and Döner R 2000 *Nature* **405** 658
[5] Yu B H, Li Y B and Tang Q B 2013 *Chin. Phys. B* **22** 013206
[6] Staudte A, Ruiz C, Schofler M, Schossler S, Zeidler D, Weber Th, Meckel M, Villeneuve D M, Corkum P B, Becker A and Dorner R 2007 *Phys. Rev. Lett.* **99** 26300
[7] Bergues B, Kūel M, Johnson N G, Fischer B, Camus N, Betsch K J, Herrwerth O, Senftleben A, Sayler A M, Rathje T, Ben-Itzhak I, Jones R R, Paulus G G, Krausz F, Moshammer R, Ullrich J and Kling M F 2012 2012 *Nat. Commun.* **3** 813
[8] Pfeiffer A N, Cirelli C, Smolarski M, Döner R and Keller U 2011 *Nat. Phys.* **7** 428
[9] Liu Y, Tschuch S, Rudenko A, Durr M, Siegel M, Morgner U, Moshammer R and Ullrich J 2008 *Phys. Rev. Lett.* **101** 053001
[10] Zhang Z, Zhang J, Bai L and Wang X 2015 *Opt. Express* **23** 7044
[11] Tate J, Auguste T, Muller H.G, Salieres P, Agostini P and DiMauro L F 2007 *Phys. Rev. Lett.* **98** 013901
[12] Gordon A and Kartner F 2005 *Opt. Express* **13** 2941
[13] Ye D, Li M, Liu J, Gong Q, Liu Y and Ullrich J 2015 *Phys. Rev. Lett.* **115** 123001
[14] Guo D S, Zhang J, Xu Z, Li X, Fu P and Freeman R R 2003 *Phys. Rev. A* **68** 043404
[15] Zhang J and Guo D S 2013 *Phys. Rev. Lett.* **110** 063002
[16] Dong S, Zhang Z, Bai L and Zhang J 2015 *Phys. Rev. A* **92** 033409
[17] Feuerstein B, Moshammer R, Fischer D, Dorn A, Schröer C D, Deipenwisch J, Crespo Lopez-Urrutia J R, Hör C, Neumayer P, Ullrich J, Rottke H, Trump C, Wittmann M, Korn G and Sandner W 2001 *Phys. Rev. Lett.* **87** 043003
[18] Haan S L and Smith Z S 2007 *Phys. Rev. A* **76** 053412
[19] Su Q and Eberly J H 1991 *Phys. Rev. A* **44** 5997
[20] Wang X, Tian J and Eberly J H 2013 *Phys. Rev. Lett.* **110** 073001
[21] Wang X and Eberly J H 2009 *Phys. Rev. Lett.* **103** 103007
[22] Wang X and Eberly J H 2012 *Phys. Rev. A* **86** 013421
[23] Mauger F, Chandre C and Uzer T 2010 *Phys. Rev. Lett.* **105** 083002
[24] Panfili R, Haan S L and Eberly J H 2002 *Phys. Rev. Lett.* **89** 113001
[25] Haan S L, Breen L, Karim A and Eberly J H 2006 *Phys. Rev. Lett.* **97** 103008
[26] Zhang J, Xie X, Roither S, Zhou Y, Lu P, Kartashov D, Schoffler M, Shafir D, Corkum P.B, Baltuška A, Staudte A and Kitzler M 2014 *Phys. Rev. Lett.* **112** 193002
[27] Zhang J, Zhang W, Xu Z, Li X, Fu P, Guo D S and Freeman R R 2002 *J. Phys. B: At. Mol. Opt. Phys.* **35** 4809
[28] ZHang X, Zhang J, Bai L, Gong Q and Xu Z 2005 *Opt. Express* **13** 8708
[29] Zhang J, Bai L, Gong S, Xu Z and Guo D S 2007 *Opt. Express* **15** 7261
[30] Ye H, Wu Y, Zhang J and Guo D S 2011 *Opt. Express* **19** 20849
[31] Wu Y, Ye H, Shao C and Zhang J 2012 *Chin. Phys. B* **2** 024210
[32] Becker A and Faisal F H M 2002 *Phys. Rev. Lett.* **89** 193003